Author/s:
Xie, K;Fu, Q;Webley, PA;Qiao, GG

Title:
MOF Scaffold for a High‐Performance Mixed‐Matrix Membrane

Date:
2018-07-09

Citation:
Xie, K., Fu, Q., Webley, P. A. & Qiao, G. G. (2018). MOF Scaffold for a High‐Performance Mixed‐Matrix Membrane. Angewandte Chemie, 130 (28), pp.8733-8738. https://doi.org/10.1002/ange.201804162.

Persistent Link:
https://hdl.handle.net/11343/285094

Author Manuscript

Title: MOF scaffold for a high performance mixed matrix membrane

Authors: Ke Xie; Qiang Fu; Paul A. Webley; Greg G. Qiao, Prof.

To be cited as: 10.1002/ange.201804162

Link to VoR: https://doi.org/10.1002/ange.201804162

MOF scaffold for a high performance mixed matrix membrane

Ke Xie,[†a] Qiang Fu,[†a] Paul A. Webley*[a] and Greg G. Qiao*[a]

[†]These authors contribute equally

Abstract: A novel composite membrane consisting of an interconnected MOF scaffold as a scaffold, coated with a cross-linked poly(ethylene glycol) (PEG), has been developed. As a result of its unique structure, the membrane shows an exceptional permeability enhancement of 18 times compared to pristine PEG membranes, without compromising the selectivity. This performance is unattainable with current mixed-matrix membranes (MMMs). Our optimized membrane has a permeability of 2,700 Barrer with CO_2/N_2 selectivity of 35, which surpasses the latest Robeson upper bound.

The separation of CO_2 from light gas mixtures (CO_2/N_2, CO_2/CH_4 etc.) by membrane technology has been intensively investigated during the past decade.[1] When compared to the traditional CO_2 capture technologies, such as physical or chemical absorption, polymeric membrane separation is more environmentally-friendly with a lower capital and operating cost,[2] as well as better processability.[2a] However, the performance of all the neat polymeric membranes are constrained by a trade-off limitation, known as "Robeson's upper bound".[3] Specifically, polymeric membranes (i.e. polyimide, polysulfone and polyethylene glycol) generally possess a low permeability and a high selectivity, or vice versa (i.e. PTMSP, polymers with intrinsic microporosity).[1-2] A mixed-matrix membrane (MMM) system consisting of a polymeric matrix and porous fillers, has been widely investigated as one pathway to overcome this limitation.[1-2]

In a typical MMM configuration, the polymer serves as a continuous phase and provides the gas separation properties by a solution-diffusion or facilitated transport mechanism. The porous filler facilitates the fast transportation of gas molecules and hence enhances gas permeability.[1-2] Different types of porous materials have been investigated as the filler for MMMs, including zeolites,[4] carbon molecular sieves,[5] graphene,[6] and metal-organic frameworks (MOFs).[7] In general, a higher filler content would lead to a higher permeability of the resultant MMMs. However, the effective filler content in MMMs for CO_2 separation is usually limited to below 40 wt.% due to the incompatibility between the matrix and fillers, which in turn results in significant brittleness of the resultant MMM. At this filler content, the enhancement of permeability in these MMMs is less than 5.4 times that of the pristine polymer. [7] In addition, the fillers were micro-sized particles or crystals in most early studies, and the morphology effect of the filler was ignored until very recently.[8] For instance, Cu-terephthalic acid (CuBDC) nanosheets were prepared by an interfacial crystallisation method and blended into polyimide to yield a MMM providing improved performance. The better performance of the morphology engineered MOFs was ascribed to the improved dispersity of 2D nanosheets in the polymer matrix.[7b] On the other hand, the morphology (particles, rod or fibres) impact of NH_2-MIL-53 has also been investigated, and the study revealed that the performance of MMMs with fibre or rod-like MOF's were identical to that of MMM incorporating normal MOF particles.[9]

Herein we report a new design of gas separation membrane possessing a hierarchical structure. An interconnected MOF scaffold (MS) was formed on a porous support, followed by coating both the surface and the gap of the entire scaffold with a crosslinked polymer to produce a gas-tight sealed membrane. Correspondingly, the resultant composite membranes are denoted as "MOF scaffold/polymer membranes (MSP)". Such membranes exhibit an enhanced CO_2 permeability 18 times greater than pristine PEG at 47 wt.% MOF content, without the compromise of selectivity. This performance also surpassed the most recent Roberson's upper bound in the permeability vs selectivity plot.

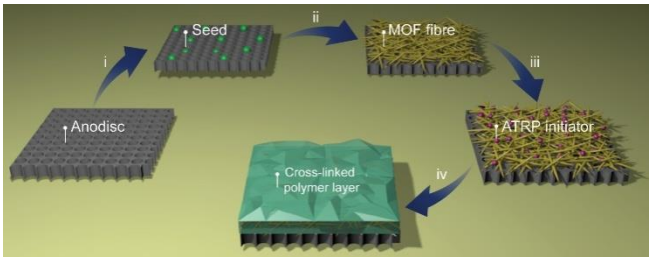

Scheme 1. Schematic illustration for the synthesis of MS layer and the MSP. i) Seeding on Anodisc; ii) formation of MS layer via secondary MOF growth; iii) functionalization of MOF fibres with BiBB; iv) polymer coating on MOF fibre surface.

[a] Prof. G. Qiao, Prof. P. A. Webley, Ke Xie and Dr. Qiang Fu
Department of Chemical Engineering
The University of Melbourne
E-mail: gregghq@unimelb.edu.au, paul.webley@unimebl.edu.au

Supporting information for this article is given via a link at the end of the document.

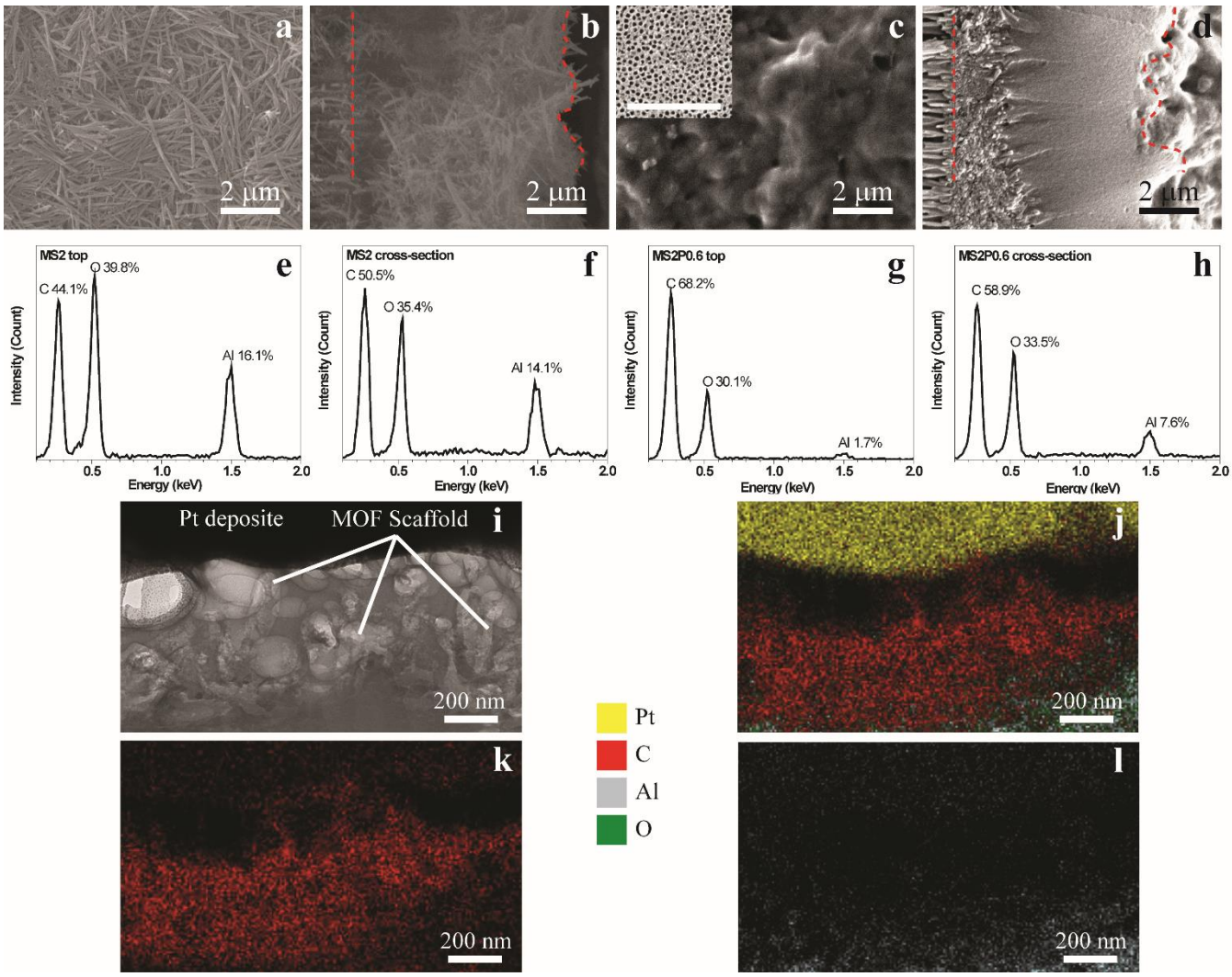

Figure 1. Reflective SEM images of MS2 (a, b) and MS2P0.6 (c, d) membranes. (a) and (c) are the top view of the membrane. (b) and (d) are the cross-section view of the membrane. The bottom view of MS2P0.6 is inset in (c), where the scale bar refers to 5 μm. e-h) the EDX spectrum acquired from the corresponding SEM images of (a-d) respectively. (i) is the TEM image of the cross-section view of the MS2P0.6 with the platinum deposited on the top. (j, k, l) are the element (Platinum- yellow; Carbon-red; Aluminium-silver; Oxygen-olive) mapping of (i).

For an ordinary MMM, the polymer matrix and filler (*e.g.* MOF) are prepared separately and then mixed together to produce the MMM. In contrast, in the present study, the MS was prepared following the procedure as shown in Scheme 1. To start with, an aluminium hydroxide/2-amino-1,4-benzenedicarboxylate ($Al(OH)_3/NH_2BDC$) particle was prepared and introduced onto the Anodisc surface as seeds for the subsequent growth of MOF fibres (step i). Thereafter the amino functionalized MS was prepared *via* a secondary growth procedure (step ii). Based on different concentration of seeds applied (0.5, 1.0 and 2.0 mg mL^{-1}), the resultant MS structures are named as MS0.5, MS1 and MS2 respectively. To demonstrate that the growth of MOF fibres is induced by the introduced $Al(OH)_3/NH_2BDC$ seeds, we carried out a series of control experiments for the MOF synthesis. The detailed experiments, results and discussion are available in supporting information SI1 and Figure S1. Based on the obtained results, we thus can conclude that the MS grows from the applied seeds and is firmly attached to the Anodisc. The study of the kinetics of MS formation was then investigated and the result is shown in Figure S2. After reacting for 72 hours, the MS layer was formed on the Anodisc. The morphology of the MS was acquired by SEM as illustrated in Figure 1 and Figure S3. From the top view of MS2 in Figure 1a, we find that the MOF fibres are densely packed, forming an interconnected sheet with fibre-like MOF crystals. The cross-sectional view of MS2 in Figure 1b suggests the thickness of this sheet is ca. 5 μm. The thickness of MS has been adjusted by changing the concentration of seeds in the seeding procedure (Scheme 1, step i). Shown in Figure S3a and S3b, the thickness of MS0.5 and MS1 is 0.6 and 1.2 μm, respectively, when using a seed concentration of 0.5 or 1.0 mg mL^{-1}, respectively.

There are two sorts of pores in the present MS: intrinsic micropores with uniform pore size within the MOF crystals, and "constructional pores" with a wide range of size distribution formed by the inter-MOF-fibre space. The intrinsic porosity of the free MOF fibre from bulk reaction for MS2 were investigated by CO_2 adsorption experiments. As plotted in Figure S4, both the free MOF fibre and MS2 showed type I isotherms and similar CO_2 uptakes. These results are in good agreement with the adsorption performance of NH_2-MIL-53 reported in the literature.[10] The cut-off size of the constructional pores was determined by a filtration experiment using a series of monodispersed particles with different diameters. The dependence of the penetrate percentage versus particle diameters is plotted in Figure S5. After the formation of MS, the cut-off size of MS is significantly reduced compared to the bare Anodisc (100 nm channel).

In this study, a surface-confined coating method, named "continuous assembly of polymer" (CAP) was adapted to form the MSP.[11] CAP technology enables formation of a crosslinked thin film with controlled thickness by combing grafting-from and grafting-to methodology. Initially, α-bromoisobutyryl bromide (BiBB) was immobilized on the MOF scaffold as the initiator for the ATRP-mediated CAP process (step iii in Scheme 1). The CAP process was then conducted by immersing the functionalized MS into an aqueous solution containing macrocross-linkers (poly(ethylene glycol) dimethacrylate, PEGDMA) and catalysts (i.e. $CuBr_2$, Me_6TREN and Na-Ascorbate) for 16 hours according to our previously reported method (step iv in Scheme 1).[11-12] It should be noted that the intrinsic porosity of the MOF fibres can be preserved after the CAP process according to our recent study.[11] A control experiment of CAP on a silicon wafer under the same conditions was performed and presented in Figure S6. The AFM analysis indicated that a 150 nm polymer film formed on the flat surface after reaction. Our previous studies on CAP thin film formation indicated that under the same preparation conditions, the CAP layer thickness on Si wafer is very close to that grown on MOF crystals (Figure S6c, S6d). Therefore this control experiment has two implications. One indicates that the coated polymer films on the surface of the MOF scaffold should be approximately 150 nm, minimizing the path length for gas diffusion into the MS. The second implication is that the cross-linked polymer can fill most of the constructional pores between the fibres (<300 nm diameters).[12-13] Any unfilled pores are likely to be isolated after the CAP process, leading to a defect-free MSP without leaks as demonstrated by the following gas separation testing.[14]

The formed MSPs are denoted by the code MSxPy where x refers to the applied seed concentration (as before) and y refers to the feed amount of PEGDMA (0.2, 0.4, 0.6 and 1.2 mmol in 5 mL aqueous solution, see Table 1). The morphologies of the MS2 based MSPs with different feed amount of PEGDMA are presented in Figure S7a (MS2P0.2), S7b (MS2P0.4) and 1c (MS2P0.6). From the evolution of the morphologies from MS2P0.2 to MS2P0.6 we can see that as the polymer feed increases, the MSs gradually lose their original appearance since the surface of the MOF fibres are coated by the amorphous polymer. The MS2P0.6 looks smooth from the top view as illustrated in Figure 1c. This result is in agreement with our previous study on the polymer coated NH_2-MIL-53 crystals.[14] The morphology of MS0.5P0.6 (Figure S3c) and MS1P0.6 (Figure S3d) are similar to MS2P0.6, and the roughness increases as the sheet thickness increases. From the cross-sectional view of the MSxPy in Figure 1d, 1i, S3e and S3f, we found that the polymer matrix almost entirely fills up the gaps between the MOF fibres, and the thickness of the product is consistent with that of the original MS layer. It is likely that the polymer matrix grows at the conjunction points between MOF fibres. Notably, the MSxPy is a type of asymmetric membrane grown above the supporting Anodisc, since the MS and the following polymerization are only achieved on the top side of the Anodisc substrate. This conclusion is confirmed by the SEM image of the bottom view of the membrane MS2P0.6 (insert in Figure 1c).

EDX scanning on the top-view and cross-sectional view of the SEM images for MS2 and MS2P0.6 membranes are presented in Figure 1e-1h. The EDX scanning on both top (Figure 1e) and cross-sectional (Figure 1f) views of the MS2 revealed an intensive aluminum composition of *ca.* 14-16 at.% assigned to the NH_2-MIL-53 (Al). After the CAP process, the aluminum ratio significantly reduces (Figure 1g, 1h) due to the coating of the polymer matrix consisting of carbon and oxygen. This result thus demonstrated the successful formation of a polymer coating on the MS. The TEM image of the cross-section view of the MS2P0.6 and corresponding element mapping are shown in Figure 1i and 1j-1k respectively, from which the structure of the MS showing different contrast and aluminum signal is observed. The TEM image also implies that the coating thickness of the polymer from the top surface of MS2P0.6 to MOF fibre is no more than 150 nm which is in good agreement with our control experiment shown in Figure S6a and S6b. The reflective membrane X-ray diffraction (XRD) spectrum of the MSx and MSxPy further confirm the formation of the cross-linked PEG layer as well as the survival of the MOF scaffold. As shown in Figure S8, MS2 exhibits sharp diffraction peaks, implying a high crystallinity of the MS, which is identified as NH_2-MIL-53. After the CAP process, we found from the XRD spectrum of MS2P0.4 that some of the peaks of NH_2-MIL-53 disperse due to the formation of CAP. MS2P0.6 with higher polymer content showed an amorphous diffraction attributed to the non-crystallized feature of the CAP which masked the crystalline peaks of the MOF.[15] The TGA results of MSx and MSxPy are provided in Figure S9 and Table S1. We found the MOF content in MSxPy varies from 37 to 47 wt.%. Table S2 lists the volume fraction of the zeolite- and MOF-based MMMs with high filler content. As seen, the volume fraction in the MS2P0.6 is close to other MMMs reported in the literature, agreeing well with MMM theoretical calculations. Based on the above characterizations, we can conclude that the configuration of this MSP is actually a composite of interconnected MOF fibre sheet and continuous polymer phase, which covers all the surface of the MS scaffold, and also fills up the constructional pores between the MOF fibres.

CO_2/N_2 separation performance of the MSPs is evaluated via the constant pressure variable volume (CPVV) method, and the results are shown in Table 1. As expected, the raw MS has high CO_2 flux of ca. 85,000 GPU with low CO_2/N_2 selectivity of ca. 0.8 due to the unsealed pores of MS. After the CAP process, the MS is covered by a polymer coating and the resultant MSP

give a CO_2 permeance of 5,400 (MS0.5P0.6), 2500 (MS1P0.6) and 560 (MS2P0.6) GPU, respectively. This observation indicates that the polymer matrix filled the constructional pores and crosslinked in-situ between the MOF fibres. The permeability of the MSxPy slightly decreases from 3,200 (MS0.5P0.6) to 3,000 (MS1P0.6) and then 2,700 (MS2P0.6) Barrer as the thickness increases. Meanwhile their CO_2/N_2 selectivity significantly increases from 2.7 (MS0.5P0.6) to 18 (MS1P0.6) and then 35 (MS2P0.6). The evolution of the membrane performance is mainly attributed to the increase of MS thickness. When the MS layer is thin (e.g. MS0.5P0.6 and MS1P0.6), the derived MSP are likely to leak, and hence resulted in higher permeability but lower selectivity. The composite membrane MS5P1.2 derived from MS5 has a low CO_2/N_2 selectivity of 5.6, indicating an unsealed polymer coating. The dependence of gas separation performance on the polymer feed concentration in the CAP process was also studied based on MS2. As shown in Table 1 and Figure 2a, when the PEGDMA feed concentration is low, the resulting membranes showed low selectivity of 2.8 and 5.0 and high CO_2 permeability of 7,340 to 3,930 Barrer for MS2P0.2 and MS2P0.4 respectively. This result reveals that in these two cases, the amount of applied polymer is insufficient to fill up the constructional pores between the MOF fibres. Once the PEGDMA feed level was increased to 0.6 mmol, the selectivity of the yielded MS2P0.6 was significantly increased to 35, indicating that a defect-free membrane was obtained. Further increase of PEGDMA feeding to 1.2 mmol provides no obvious enhancement of the membrane performance. This result can be attributed to the 'buried' effect, which limits the maximum thickness achieved by the CAP method.[12]

To demonstrate the necessity of the ***in-situ*** formation of MS, a composite membrane was prepared by filtering the dispersion of MOF fibres through an Anodisc, followed by the CAP process under the same conditions. This approach resulted in a non-selective composite membrane as shown in Figure S10.

Figure 2b plots the CO_2/N_2 separation performance of the MS1P0.6 and MS2P0.6 membranes as well as the pristine PEG-based dense membrane prepared via a similar approach.[12] In addition, PEG based membranes and other MMMs reported in the literature are plotted for comparison. From Figure 2b we see that the performance of the MS2P0.6 is comparable to the state-of-the-art non-facilitated transport membranes and surpasses the latest upper bound in this field. The CO_2 permeability of MS2P0.6 (2,700 Barrer) is ~18 times higher than that of the pristine PEG membrane (ca. 140 Barrer) with a MOF content of 47%. Such a dramatic improvement has never been achieved by ordinary MMM systems through blending approaches. In general, for conventional MMM's, the enhancement of permeability is no more than 5.4 times (see Table S2 in supporting information) even for those CO_2 separation MMMs having high content of filler at 40%. This unusual result may be attributed to the unique configuration of the MS architecture. Firstly, the filler (NH_2-MIL-53) content in the present membrane system (~47 wt.%) is much higher than that in most of the NH_2-MIL-53 based gas separation MMMs (up to ca. 25 wt.%).[7c, 9] It is well-known that ordinary MMMs suffer from significant issues, such as filler incompatibility and aggregation, which limit their tolerance to high filler content. In contrast, the polymer coating conducted here, is formed by grafting macro cross-linker from the surface of the MOF fibres via CAP process in this strategy. This allows for a chemical integration of polymer and MOF components and hence avoids the issues of incompatibility and aggregation, regardless of the high filler content. We simulated the gas separation performance of MMMs using the well-established Maxwell theory (SI4 in supporting information).[16] This analysis indicates that if the filler content is able to increase to 47 wt.% (or 74% vol.% in this case), the permeability should be enhanced by only 8 times. Therefore, we hypothesize that the unique architecture of the MOF filer (interconnected fibres) as well as the high MOF content are responsible for the significant enhancement in CO_2 permeability (18 times) for these MSP.

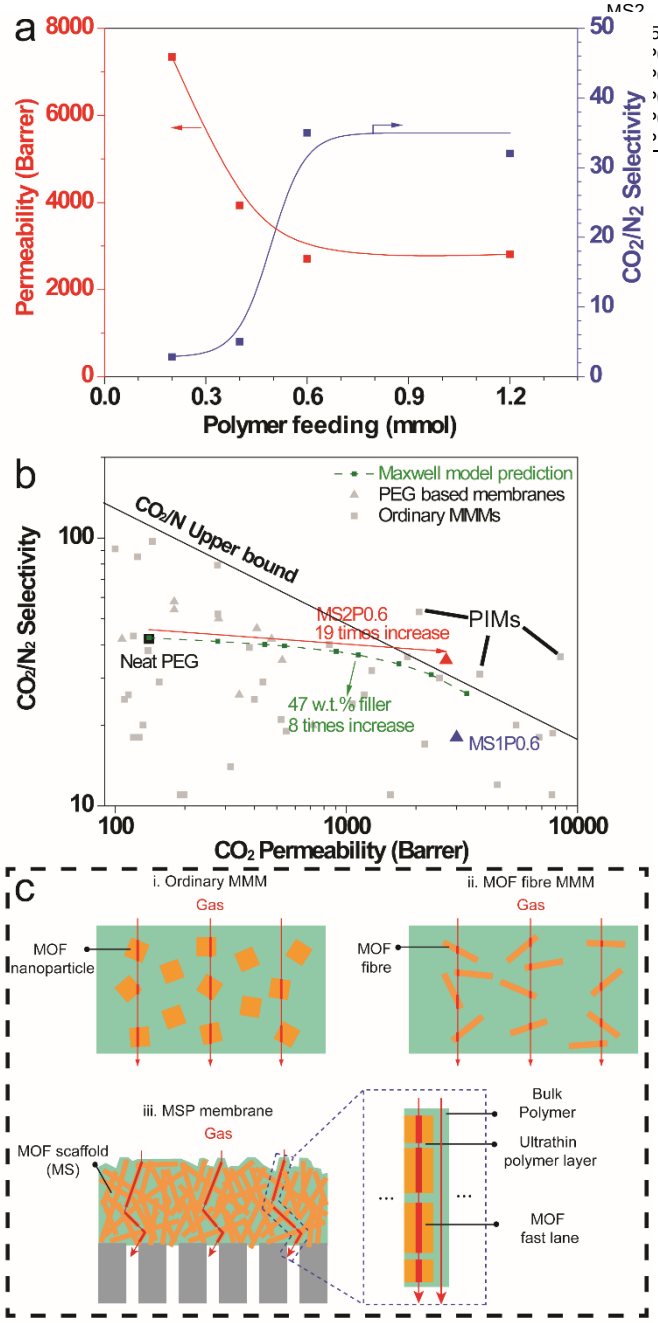

Figure 2. (a) The dependence of membrane performance on the PEGDMA applied in the CAP process. (b) The selectivity vs. permeability diagram. The performance of PEG based membranes (grey triangle) and ordinary MMMs (grey square) are plotted for comparison.[1] The green dashed line is the calculated MMM performance based on the Maxwell equation. (c) The schematics representing the different gas transport mechanism in MOF nanoparticle (Case i) blended MMMs, MOF fibre (Case ii) blended MMMs, and the present MSP (Case iii). The red line refers to the pathway for gas transport across the membrane in which the width represents the gas transport rate (wider line refers to higher rate).

Table 1 CO_2/N_2 separation performance of MS2 and MSxPy (x refers to seed concentration and y refers to total polymer feed level).

Sample	Thickness (μm)	MOF content	Permeance (GPU)	Permeability (Barrer)	CO_2/N_2 Selectivity
MS2	5.1	100 wt. %	~ 85,000	n/a	~1
5P0.6	0.6	—	5,400±450	3,200±270	2.7±0.4
0.6	1.2	37.0 wt. %	2,500±200	3,000±200	18±2
0.2	4.8	—	1,530	7,340	2.8
0.4	5.1	—	770	3,930	5.0
0.6	4.9	47.4 wt. %	560±40	2,700±200	35±3
1.2	5.2	—	540±30	2,810±150	32±3

Some studies on such co-continuous like materials indicate a significant enhancement on mass transport (e.g. water, ions).[17] A schematic showing the gas transport mechanisms in different configurations of MMMs is shown in Figure 2c. For ordinary MMMs using either MOF nanoparticles or fibres (case i or ii), the gas molecule alternatively passes through the matrix and filler phases, whose behaviour can be well fitted with the Maxwell equation. This speculation has been proved by the previous study on NH_2-MIL-53/polyimide MMMs.[9] By contrast, in the present MSP (case iii), the MOF fibres formed a continuous sheet prior to the polymer coating. With this configuration, the resultant membranes are actually performing better than the Maxwell equation predicted since Maxwell theory doesn't account for the effect of an interconnected structure of filler. The interconnected structure of the porous MOF fibres can facilitate fast transportation of the gas molecules all the way through the majority of the membrane, leading to significant enhancement of permeability. On the other hand, the thin PEG-based polymer coating (<150 nm) on the MS fibres can maintain the selectivity (20 to 50) for CO_2 over N_2 separations.[11-12] The actual primary gas transport model in these membranes can be simulated as a series of $(PEG/MOF)_n$ layers (Figure 2c, case iii). Through a theoretical estimation (SI4 in supporting information), in order to achieve a 18 times enhancement of permeability, the effective MOF content in ordinary MMM would have to be >90 wt.% (or 96 vol.%), which is 1.9 times that of the real overall MOF content in the MSP (47 wt%).

The CO_2/N_2 separation performance of the MS2P0.6 was also tested using a 10%CO_2/90%N_2 (v./v.) mixed gas, showing a lower CO_2 permeability of 1,830 Barrer while maintaining a CO_2/N_2 selectivity of 32 (which is expected from the mix gas tests). The MS2P0.6 keeps its integrity at the pressure as high as 3.5 MPa in a mechanical compression test, and the optimised operational pressure is of below 400 kPa due to the fracture of Anodisc. MS2P0.6 is mechanically strong enough for the application in post-combustion CO_2 separation due to the modest pressure of this application.[18] After exposure to lab conditions (air, room temperature) for 30 days, the MS2P0.6 presented relatively stable gas separation performance (permeability increase by 2%, and selectivity decreased by 9%) because the high permeability of MSPs comes from the stable and rigid MOF scaffold structure. This excellent stability is superior to ordinary high permeability polymeric materials such as polymer of intrinsic microporosity (PIM) and poly(1-trimethylsilyl-1-propyne) (PTMSP), for which the permeability decays by 30~90% under similar conditions due to ageing.[19]

In summary, MSPs, consisting of MOF and polymer components with co-continuous-like phase, were fabricated based on MS via the CAP process. The optimized membrane shows promising CO_2/N_2 separation performance with a CO_2 permeability of 2,700 Barrer and a selectivity of 35 owing to their rational hierarchical structure. The continuous MS in the

composite membrane facilitates fast gas transport that can enhance the gas permeability by over 18 times in comparison with the pristine polymer. This work thus opens up a new avenue for the development of composite membrane systems for efficient gas separation applications.

Experimental Section

Materials; control experiment for MOF synthesis; characterizations; gas separation tests can be found in Supporting Information.

Preparation of $Al(OH)_3/NH_2$-BDC seed: 1.5 g of $Al(NO_3)_3{\cdot}9H_2O$ and 1.0 g of PEO-PPO-PEO were dissolved in 30 mL DI-water. Into this solution the diluted ammonia solution was added dropwise until pH=9. The $Al(OH)_3$ nanoparticles were purified by centrifuge, washed by DI-water and dispersed in DMF to obtain a 2.0 mg mL^{-1} dispersion. 0.24 g of (NH_2-BDC) was then dissolved in 40 mL of $Al(OH)_3$/DMF dispersion, sealed in a Teflon-lined autoclave and heated to 120 ^oC for 24 hours to yield yellow $Al(OH)_3/NH_2$-BDC nanoparticle seeds. The seeds were purified by centrifuge, washed by DMF and dispersed in THF.

Formation of MOF scaffold (MS) on Anodisc: The MS was prepared via a secondary growth approach. In a typical synthesis, a piece of Anodisc (ϕ13 mm, 100 nm channel) was dip-seeded in seed/THF dispersion with different concentrations (0.5, 1.0 and 2.0 mg mL^{-1}) and dried in air. The reaction solution was prepared by dissolving 0.10 g $Al(NO_3)_3{\cdot}9H_2O$ and 0.14 g NH_2-BDC into 15 mL DMF. The seeded Anodisc was placed onto a glass substrate that was pre-wetted by the reaction solution and the air bubbles were removed carefully so the disc was firmly pressed on the glass wafer by the capillary force. Then the glass wafer loaded disc was placed on the bottom of a Teflon-lined autoclave, and the crystallization was conducted at 130 ^oC for 72 hours. After the reaction, the colour of the disc changed from white to yellow. The disc was sonicated in methanol (5 minutes × 3) to remove excess ligand and loose MOF crystals. The MOF/Anodisc was dried in vacuum at 60 ^oC overnight before the next step. Based on the seed concentration, the obtained MOF membranes are named as MS0.5 (0.5 mg mL^{-1}), MS1 (1.0 mg mL^{-1}) and MS2 (2.0 mg mL^{-1}).

Formation of MSPs (MSxPy): The PEG based polymer was crosslinked *via* the ATRP of poly(ethylene glycol) dimethacrylate (PEGDMA, 550 Da, as the macro-crosslinker).[11-12, 20] In a normal procedure, PEGDMA (330 mg, 0.6 mmol), $CuBr_2$ (1.1 mg, 0.005 mmol), Tris[2-(dimethylamino)ethyl] amine (Me_6Tren, 1.33 µL, 0.005 mmol) and sodium ascorbate (3 mg, 0.015 mmol) were dissolved in 5 mL DI-water. The Br-MSs were placed into this solution, attached onto the top of an Eppendorf ThermoMixer C and were shaken at room temperature for 16 hours. After the reaction, the membrane was rinsed in DI-water and dried in a vacuum at room temperature overnight before gas separation measurements.

Acknowledgement

The authors appreciate the Bio21 Advanced microscopy facility for the assistance of materials characterization.

Keywords: poly ethylene oxide • one dimensional MOF • polymer MOF composite • co-continuous • MOF non-woven cloth

[1] S. Wang, X. Li, H. Wu, Z. Tian, Q. Xin, G. He, D. Peng, S. Chen, Y. Yin, Z. Jiang, *Energy Environ. Sci.* **2016**, *9*, 1863-1890.

[2] a) T.-S. Chung, L. Y. Jiang, Y. Li, S. Kulprathipanja, *Prog. Polym. Sci.* **2007**, *32*, 483-507; b) M. Rezakazemi, A. E. Amooghin, M. M. Montazer-Rahmati, A. F. Ismail, T. Matsuura, *Prog. Polym. Sci.* **2014**, *39*, 817-861.

[3] L. M. Robeson, *J. Membr. Sci.* **2008**, *320*, 390-400.

[4] Y. Li, H.-M. Guan, T.-S. Chung, S. Kulprathipanja, *J. Membr. Sci.* **2006**, *275*, 17-28.

[5] J. Zhang, J. A. Schott, Y. Li, W. Zhan, S. M. Mahurin, K. Nelson, X.-G. Sun, M. P. Paranthaman, S. Dai, *Adv. Mater.* **2017**, *29*, 1603797.

[6] M. Karunakaran, R. Shevate, M. Kumar, K.-V. Peinemann, *Chem. Commun.* **2015**, *51*, 14187-14190.

[7] a) T.-H. Bae, J. R. Long, *Energy Environ. Sci.* **2013**, *6*, 3565-3569; b) T. Rodenas, I. Luz, G. Prieto, B. Seoane, H. Miro, A. Corma, F. Kapteijn, F. X. L. i Xamena, J. Gascon, *Nature materials* **2015**, *14*, 48-55; c) J. E. Bachman, J. R. Long, *Energy Environ. Sci.* **2016**, *9*, 2031-2036; d) M. W. Anjum, F. Vermoortele, A. L. Khan, B. Bueken, D. E. De Vos, I. F. Vankelecom, *ACS Appl. Mater. Inter.* **2015**, *7*, 25193-25201; e) J. Dechnik, J. Gascon, C. Doonan, C. Janiak, C. J. Sumby, *Angew. Chem. Int. Ed.* **2017**, *56*, 9292-9310.

[8] a) I. Stassen, M. Styles, T. Van Assche, N. Campagnol, J. Fransaer, J. Denayer, J.-C. Tan, P. Falcaro, D. De Vos, R. Ameloot, *Chem. Mater.* **2015**, *27*, 1801-1807; b) N. Campagnol, I. Stassen, K. Binnemans, D. E. de Vos, J. Fransaer, *J. Mater. Chem. A* **2015**, *3*, 19747-19753.

[9] A. Sabetghadam, B. Seoane, D. Keskin, N. Duim, T. Rodenas, S. Shahid, S. Sorribas, C. L. Guillouzer, G. Clet, C. Tellez, *Adv. Funct. Mater.* **2016**.

[10] F. Zhang, X. Zou, X. Gao, S. Fan, F. Sun, H. Ren, G. Zhu, *Adv. Funct. Mater.* **2012**, *22*, 3583-3590.

[11] K. Xie, Q. Fu, J. Kim, H. Lu, Y. He, Q. Zhao, J. Scofield, P. A. Webley, G. G. Qiao, *J. Membr. Sci.* **2017**.

[12] Q. Fu, J. Kim, P. A. Gurr, J. M. Scofield, S. E. Kentish, G. G. Qiao, *Energy Environ. Sci.* **2016**, *9*, 434-440.

[13] Y. Zhang, A. M. Avila, B. Tokay, H. H. Funke, J. L. Falconer, R. D. Noble, *J. Membr. Sci.* **2010**, *358*, 7-12.

[14] K. Xie, Q. Fu, C. Xu, H. Lu, Q. Zhao, R. Curtain, D. Gu, P. A. Webley, G. G. Qiao, *Energy Environ. Sci.* **2018**, *11*, 544-550.

[15] a) K. Xie, Q. Fu, Y. He, J. Kim, S. Goh, E. Nam, G. Qiao, P. Webley, *Chem. Commun.* **2015**, *51*, 15566-15569; b) T. Rodenas, M. van Dalen, P. Serra-Crespo, F. Kapteijn, J. Gascon, *Microporous Mesoporous Mater.* **2014**, *192*, 35-42.

[16] T. T. Moore, R. Mahajan, D. Q. Vu, W. J. Koros, *AIChE J.* **2004**, *50*, 311-321.

[17] a) M. Lavorgna, G. Mensitieri, G. Scherillo, M. T. Shaw, S. Swier, R. A. Weiss, *J. Polym. Sci., Part B: Polym. Phys.* **2007**, *45*, 395-404; b) J. Bae, Y. Li, J. Zhang, X. Zhou, F. Zhao, Y. Shi, J. Goodenough, G. Yu, *Angew. Chem.* **2018**; c) M. Zhou, P. R. Nemade, X. Lu, X. Zeng, E. S. Hatakeyama, R. D. Noble, D. L. Gin, *J. Am. Chem. Soc.* **2007**, *129*, 9574-9575; d) E. S. Hatakeyama, B. R. Wiesenauer, C. J. Gabriel, R. D. Noble, D. L. Gin, *Chem. Mater.* **2010**, *22*, 4525-4527; e) B. M. Carter, B. R. Wiesenauer, R. D. Noble, D. L. Gin, *J. Membr. Sci.* **2014**, *455*, 143-151.

[18] T. C. Merkel, H. Lin, X. Wei, R. Baker, *J. Membr. Sci.* **2010**, *359*, 126-139.

[19] a) N. Morlière, C. Vallières, L. Perrin, D. Roizard, *J. Membr. Sci.* **2006**, *270*, 123-131; b) P. Bernardo, F. Bazzarelli, F. Tasselli, G. Clarizia, C. Mason, L. Maynard-Atem, P. Budd, M. Lanč, K. Pilnáček, O. Vopička, *Polymer* **2017**, *113*, 283-294; c) G. Consolati, I. Genco, M. Pegoraro, L. Zanderighi, *Journal of Polymer Science-B-Polymer Physics Edition* **1996**, *34*, 357-368.

[20] H. Cheng, P. Wang, J. Luo, J. Fransaer, D. E. De Vos, Z.-H. Luo, *Ind. Eng. Chem. Res.* **2015**, *54*, 3107-3115.

Table of Contents
COMMUNICATION

MOF scaffold (MS): a hierarchical MOF structure leading to unexpected significant enhancement of membrane permeability in mixed matrix membrane.

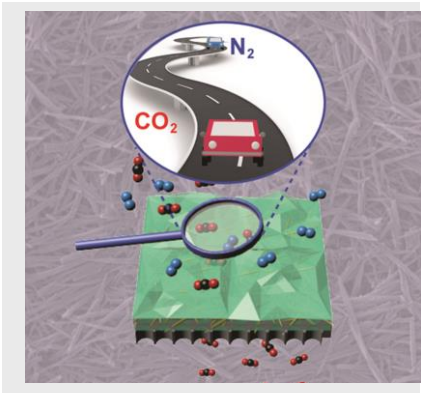

Ke Xie,[†] Qiang Fu,[†] Paul A. Webley and Greg G. Qiao**

Page No. – Page No.

MOF scaffold for a high performance mixed matrix membrane